Earthline Journal of Chemical Sciences
E-ISSN: 2581-9003; CODEN: EJCSB4
Volume 13, Number 2, May 2026, Pages 173-185
https://doi.org/10.34198/ejcs.13226.13.173185

Some acetylpenicillamines – DFT treatment

Lemi Türker

Department of Chemistry, Middle East Technical University, Üniversiteler, Eskişehir Yolu No: 1, 06800 Çankaya/Ankara, Turkey
e-mail: lturker@gmail.com; lturker@metu.edu.tr

Abstract

Presently, N-, O- and S-acetyl-substituted penicillamines have been considered within the constraints of density functional theory at the level of B3LYP/6-311++G(d,p). Some of the species have isomeric and some diasteromeric relationship with each other. N-acetylpenicillamine has some medical use as a chelating agent for many metal poisoning cases such as mercury, copper etc. (Wilson's disease is to be mentioned). The presently collected data have revealed that the optimized structures of them have exothermic heats of formation and favorable Gibbs free energy of formation values. They are thermally favored and electronically stable at the standard states. Various structural and quantum chemical data have been collected and discussed, including UV-VIS spectra. Many data obtained are dictated not only by the gross and fine topological factors but also the configuration of the species considered.

1. Introduction

For treatment, mercury-binding compounds augment excretion of the metal in intoxicated patients regardless of the type of mercury exposure. The agents employed include d-penicillamine, *N*-acetyl-DL-penicillamine, and thiol resins. Dimer-caprol (BAL) is no longer utilized, because it increased the cerebral mercury concentrations in animals experimentally receiving the methyl form. Administration of chelating agents results in only irregular removal of mercury from the body. When chelating agents are administered, mercury concentrations of blood increase for 1–3 days, presumably as a result of rapid mobilization from the tissues and a slower rate of urinary and fecal excretion. After this period, blood concentrations decline. Thiol resins are not absorbed from the gastrointestinal tract, so they can be administered orally to bind mercury in bile and other fluids within the intestine. Fecal excretion is then enhanced by preventing reabsorption of methyl mercury so that redistribution of mercury in the body will not occur. Because thiol resins cannot reenter the body, they have no potentially adverse systemic effects. Spironolactone has also been employed in the experimental treatment of inorganic mercury poisoning. The protective effect appears to be related to increasing stool excretion through a yet unknown mechanism.

N-Acetyl-DL-penicillamine is a chelating agent [1-3]. It inhibits the binding of methyl mercury to isolated human erythrocytes by 50% and removes 50% of methyl mercury ions from methyl mercury-loaded blood cells when used at a concentration of 1 mM [1,2]. N-Acetyl-DL-penicillamine (3 mmol/kg per day) reduces the biological half-life of mercury and decreases liver, kidney, brain, and blood mercury levels, as well as increases urinary excretion of mercury in a concentration-dependent manner, in mice when administered following injection of methyl mercuric chloride. It decreases mercuric chloride-induced mortality in mice when administered orally at a dose of 1.6 mmol/kg [3]. N-Acetyl-DL-penicillamine is also an analog of SNAP

Received: March 15, 2026; Accepted: April 15, 2026; Published online: April 20, 2026

Keywords and phrases: penicillamine, acetylpenicillamines, chelating agent, isomers, DFT calculations.

(S-nitroso-N-acetyl-penicillamine) that does not generate nitric oxide and has been used as a negative control in experiments using SNAP [4,5].

D-Penicillamine is a degradation product of penicillin that can utilize nitrogen, oxygen, or sulfur atoms as donors. It is an effective chelating agent for lead (II), mercury (II) and copper (II) and for many other metals. N-acetyl-D-penicillamine is less toxic than D-penicillamine and both reagents can be administered orally. D-penicillamine has been used in treatment of rheumatism, arthritis and cystinuria. It is the preferred treatment for Wilson's disease, severe active rheumatoid arthritis, and cystinuria. It works by binding to excess copper, cystine, or heavy metals to facilitate their excretion, and by suppressing immune system activity and both penicillamines have been used against mercury with the N-acetyl derivative being very effective at removing methyl mercury (II) from brain tissue. Caution must be exercised with the use of both BAL and D-penicillamine with cadmium (II) as the complexes formed are more toxic than the metal [6].

SNAP (S-Nitroso-N-acetyl-penicillamine) is an S-nitrosothiol and is used as a model for the general class of *S*-nitrosothiols which have received much attention in biochemistry because nitric oxide and some organic nitroso derivatives serve as signaling molecules in living systems, especially related to vasodilatation [7]. SNAP is derived from the amino acid penicillamine. S-Nitrosoglutathione is a related agent.

Various articles exist in the literature about the penicillamines and their derivatives [8-13]. In the present treatise, acetyl on N-, O- or S-substituted penicillamines are considered.

2. Method of Calculations

In the present study, all the initial optimizations of the structures leading to energy minima have been achieved first by using MM2 method which is then followed by semi empirical PM3 self consistent fields molecular orbital method [14-16]. Afterwards, the structure optimizations have been achieved within the framework of Hartree-Fock and finally by using density functional theory (DFT) at the level of B3LYP/6-311++G(d,p) [17,18]. Note that the exchange term of B3LYP consists of hybrid Hartree-Fock and local spin density (LSD) exchange functions with Becke's gradient correlation to LSD exchange [19]. The correlation term of B3LYP consists of the Vosko, Wilk, Nusair (VWN3) local correlation functional [20] and Lee, Yang, Parr (LYP) correlation correction functional [21]. In the present study, the normal mode analysis for each structure yielded no imaginary frequencies for the $3N–6$ vibrational degrees of freedom, where N is the number of atoms in the system. This search has indicated that the structure of each molecule considered corresponds to at least a local minimum on the potential energy surface. Furthermore, all the bond lengths have been thoroughly searched in order to find out whether any bond cleavages occurred or not during the geometry optimization process. All these computations were performed by using SPARTAN 06 program [22].

3. Results and Discussion

Figure 1 shows some diastereoisomers (R and S forms) of N-acetyl-penicillamines in which acetyl group is attached to N, O or S atom in each case. Note that R and S forms of diastereoisomers shown in the figure stand for L and D forms of N-acetyl-penicillamines, respectively.

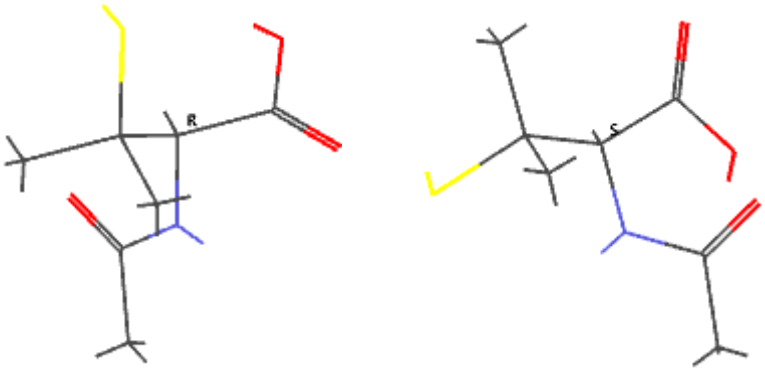

Figure 1. R and S forms (L and D, respectively) of N-acetyl-penicillamines.

Figure 2 and 3 show the optimized structures and the direction of dipole moment vectors of the species considered. Note the point of attachment in each case. Structures in Figure 2, all possess R-configuration whereas in Figure 3 they have S-configuration.

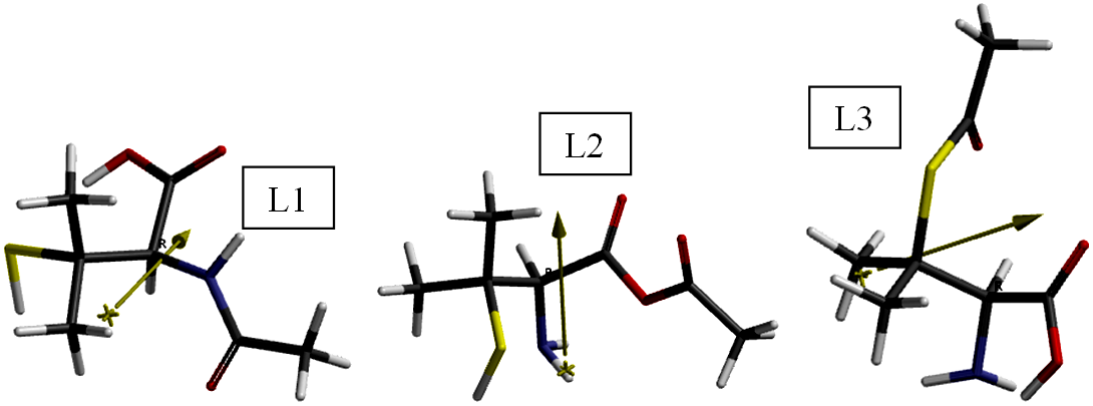

Figure 2. Optimized structures of N-, O- and S-acetyl-L-penicillamines considered (all have R-configuration).

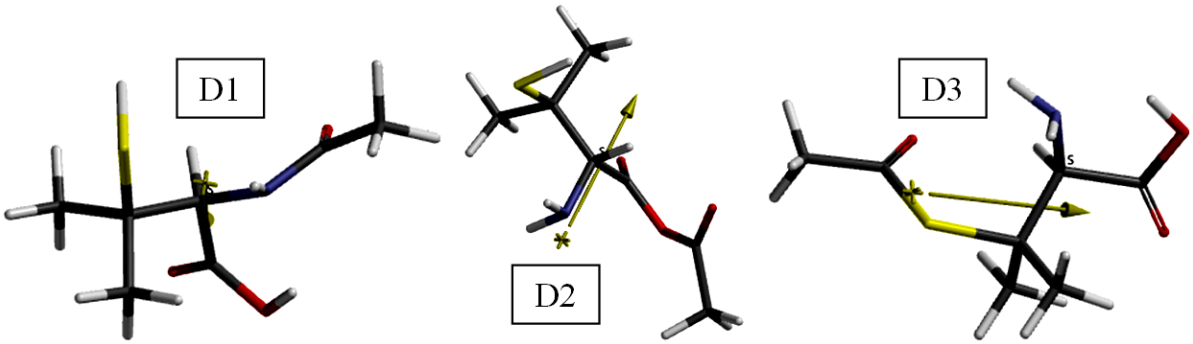

Figure 3. Optimized structures of N-, O- and S-acetyl-D-penicillamines considered (all have S-configuration).

Table 1 lists some thermo chemical properties of the species considered. The data in table reveal that the standard heat of formation (H^o) values of the species are exothermic and they are favored according to their G^o (Gibbs free energy of formation) values. As seen in the table N-acetyl derivatives (irrespective of the character of L/R or D/S) are more exothermic and more favored than the others.

Table 1. Some thermo chemical properties of the species considered.

Structure/ configuration	Acetyl linkage	H^o	S^o (J/mol^o)	G^o
L1/R	N-	-2502674.633	442.57	-2502806.584
L2/R	O-	-2502607.958	452.20	-2502742.784
L3/R	S-	-2502621.222	448.77	-2502755.024
D1/S	N-	-2502657.546	445.76	-2502790.450
D2/S	O-	-2502604.374	451.23	-2502738.909
D3/S	S-	-2502634.531	445.69	-2502767.414

Energies in kJ/mol.

Table 2 shows some energies of the species considered. Note that E, ZPE and E_C stand for the total electronic energy, zero point vibrational energy and the corrected total electronic energy, respectively [22]. The data in the table reveal that N-acetyl derivatives electronically more stable than the O- and S-acetyl substituted forms (namely, N-> S-> O-).

Table 2. Some energies of the species considered.

Structure/ configuration	Acetyl linkage	E	ZPE	E_C
L1/R	N-	-2503214.20	528.46	-2502685.74
L2/R	O-	-2503143.74	523.41	-2502620.33
L3/R	S-	-2503163.86	530.73	-2502633.13
D1/S	N-	-2503196.04	527.00	-2502669.04
D2/S	O-	-2503141.13	524.34	-2502616.79
D3/S	S-	-2503177.77	531.68	-2502646.09

Energies in kJ/mol.

Aqueous energies of the species considered are shown in Table 3. Many factors collectively contribute for the aqueous energies. However, if one considers the isomeric pairs only, the only difference comes from the configuration, and then the conclusion is that R-form is more favored than the respective S-form in terms of the aqueous energy.

Table 3. Aqueous energies of the species.

L1/R	L2/R	L3/R	D1/S	D2/S	D3/S
-2503242.03	-2503172.87	-2503215.37	-2503231.02	-2503162.02	-2503210.13

Energies in kJ/mol.

Figures 4 and 5 display the electrostatic potential (ESP) charges on atoms of presently considered structures. Note that the ESP charges are obtained by the program which uses a numerical method that generates charges, thus reproducing the electrostatic potential field from the entire wavefunction [22].

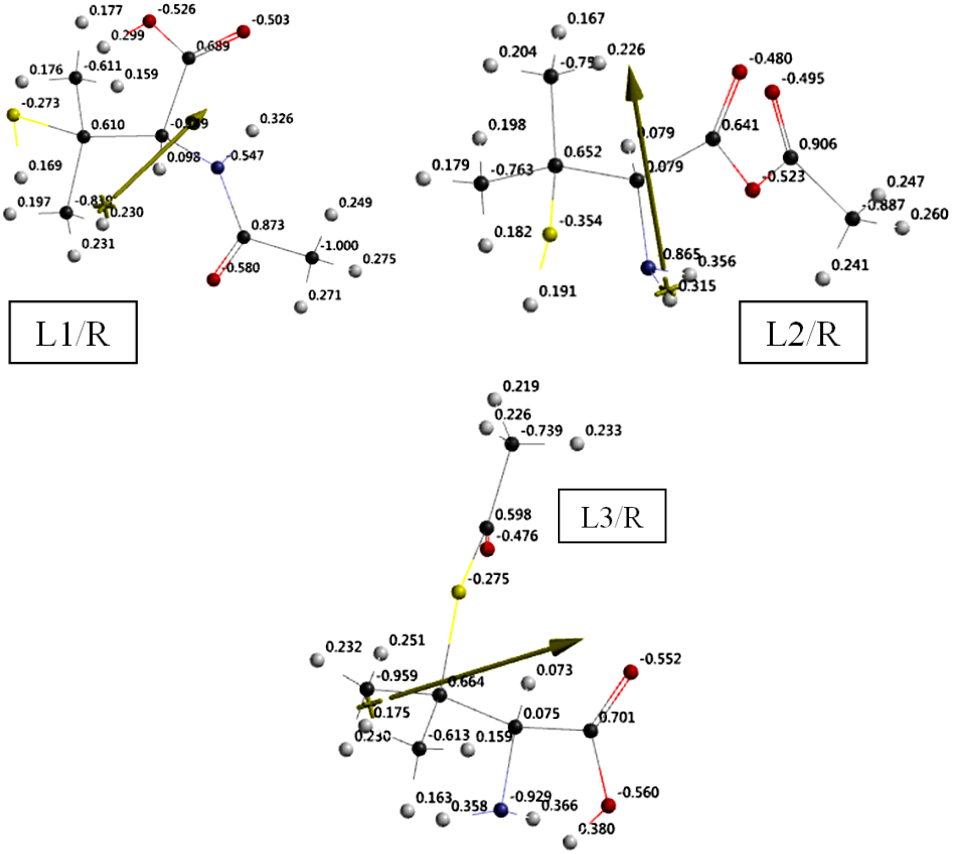

Figure 4. ESP charges on atoms of structures L1/R-L3/R.

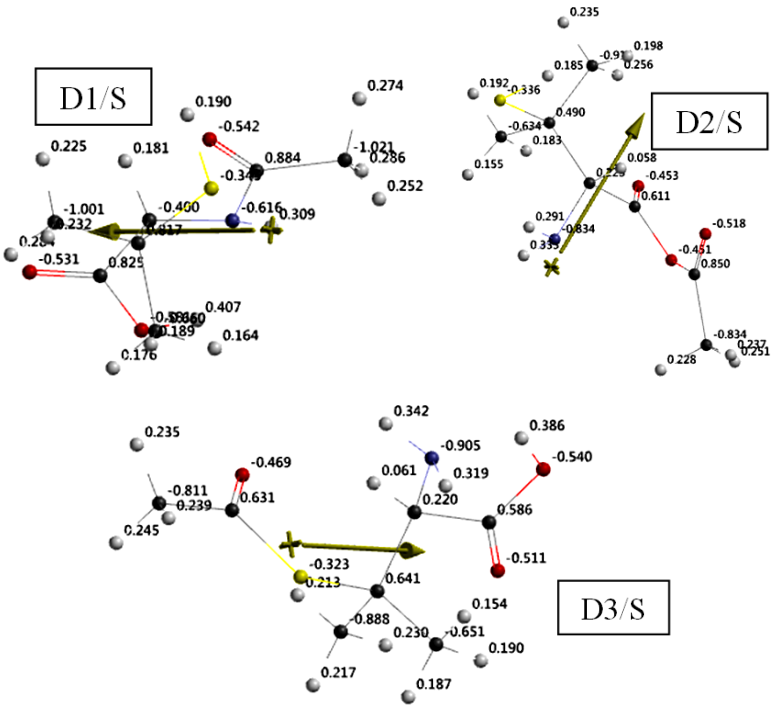

Figure 5. The ESP charges on atoms of structures D1/R-D3/R.

Figure 6 stands for the chemical function descriptors (CFD) of the structures considered. Note that CFDs are attributes given to a molecule in order to characterize or anticipate its chemical behavior. In the figure different colors stand for different descriptors. Note that HBA and HBD mean hydrogen bond acceptors and donors, respectively. Both of the structural isomers have the same number of the same kind of CFDs. Therefore, differences in properties of them should arise from the minor differences in the gross and fine topologies of the structures. The CFDs give an idea in designing molecular structure for some special usage in structure-activity relationships such as Log P values (see below).

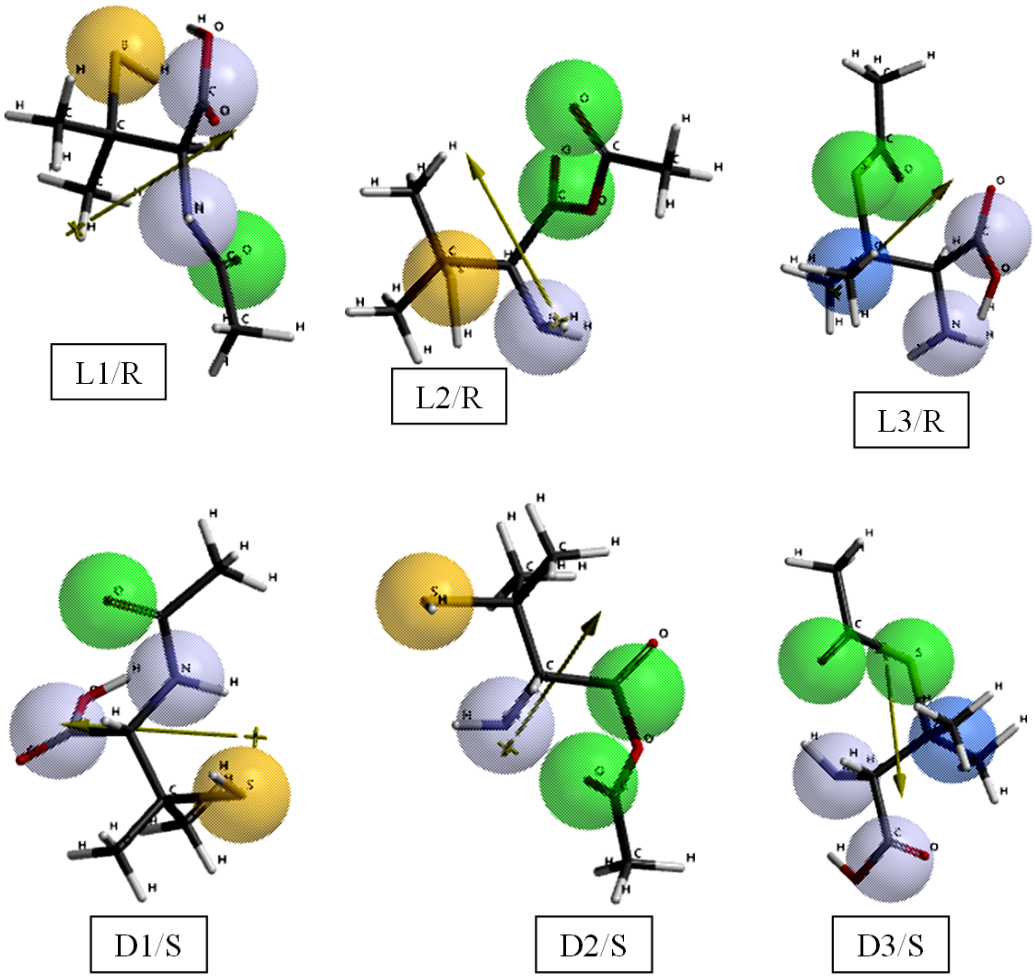

Figure 6. CFDs of the species considered (Green: HBA; Yellow: HBA and HBD; Blue: Hydrophobe; Bluish: HBA, HBD and +ionizable).

Table 4 lists some calculated properties of the species considered**.** The dipole moment values of the species steadily increase except D2/S case. The log P values exhibit algebraic decrease and increase having no regular order.

Partition coefficients are important property and useful in estimating the distribution of drugs within the body. Hydrophobic drugs with high octanol-water partition coefficients are mainly distributed to hydrophobic areas such as lipid bilayers of cells. Conversely, hydrophilic drugs (low octanol/water partition coefficients) are found primarily in aqueous regions such as blood serum. Note that the log P values of these species vary in a narrow range.

Table 4. Some calculated properties of the species considered**.**

Structure/ configuration	Eaq (kJ/mol)	Dipole (debye)	Log P	Polarizability	Cv (J/mol^o)
L1/R	-2503242.03	2.86	-0.45	54.75	156.63
L2/R	-2503172.87	3.46	-0.41	55.19	158.08
L3/R	-2503215.37	4.40	-0.42	54.94	157.10
D1/S	-2503231.02	5.57	-0.45	54.86	157.55
D2/S	-2503162.02	1.70	-0.41	55.13	158.19
D3/S	-2503210.13	5.81	-0.42	54.98	156.95

Polarizabilities in 10^{-30} m^3 units

On the other hand, the polarizability is defined according to the formula [22].

$$\text{Polarizability} = 0.08*V - 13.0353*h + 0.979920*h^2 + 41.3791$$

where V and h are the Van der Waals volume and hardness, respectively. Hardness is defined as,

$$\text{Hardness} = -(\varepsilon_{HOMO} - \varepsilon_{LUMO})/2$$

Table 5 shows some other calculated properties of the species considered. Polar surface area (PSA) is defined as the amount of molecular surface area arising from polar atoms (N,O) together with their attached hydrogen atoms. Molecules with PSA values greater than 140 $Å^2$ tend to be poor at permeating cell membranes whereas to penetrate the blood-brain barrier a PSA value of a molecule should be less than 90 $Å^2$ [23,24].

Table 5. Some other calculated properties of the species considered.

Structure/ configuration	Area ($Å^2$)	Volume ($Å^3$)	Ovality	PSA ($Å^2$)	Tautomers
L1/R	210.83	184.26	1.35	53.373	3
L2/R	220.32	186.20	1.40	59.109	0
L3/R	210.20	184.87	1.34	66.428	1
D1/S	213.16	184.89	1.36	54.222	3
D2/S	214.02	185.65	1.36	55.491	0
D3/S	210.33	185.05	1.34	66.130	1

They all belong to C1 point group.

Figure 7 shows the electrostatic potential maps of the species considered where negative potential regions reside on red/reddish and positive ones on blue/bluish parts of the maps.

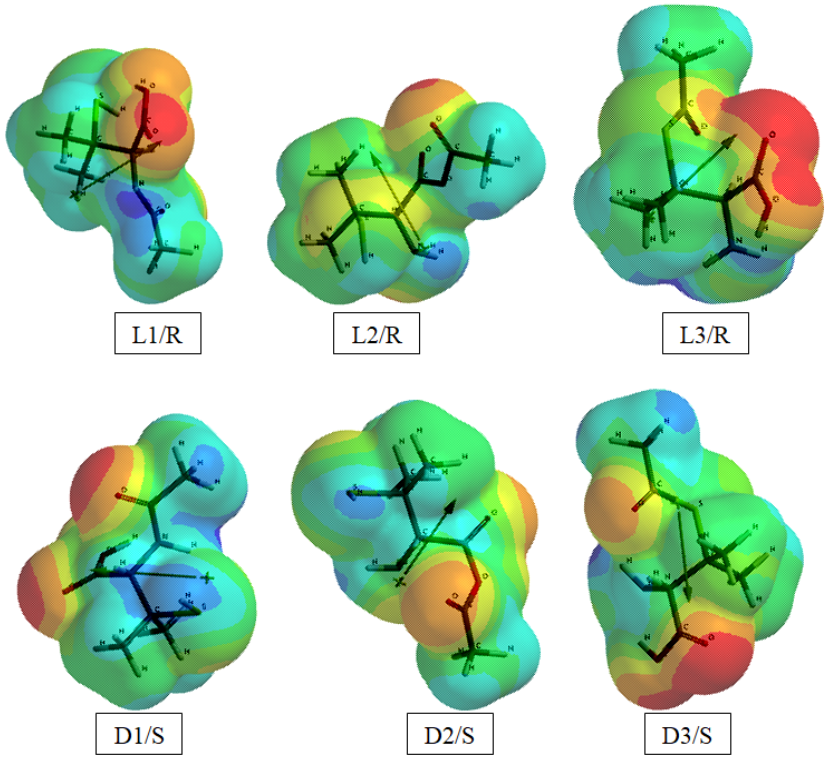

Figure 7. The electrostatic potential maps of the species considered.

Figure 8 shows the local ionization potential maps of the species where conventionally red/reddish regions (if any exists) on the density surface indicate areas from which electron removal is relatively easy, meaning that they are subject to electrophilic attack. Note that the local ionization potential map is a graph of the value of the local ionization potential on an isodensity surface corresponding to a van der Waals surface.

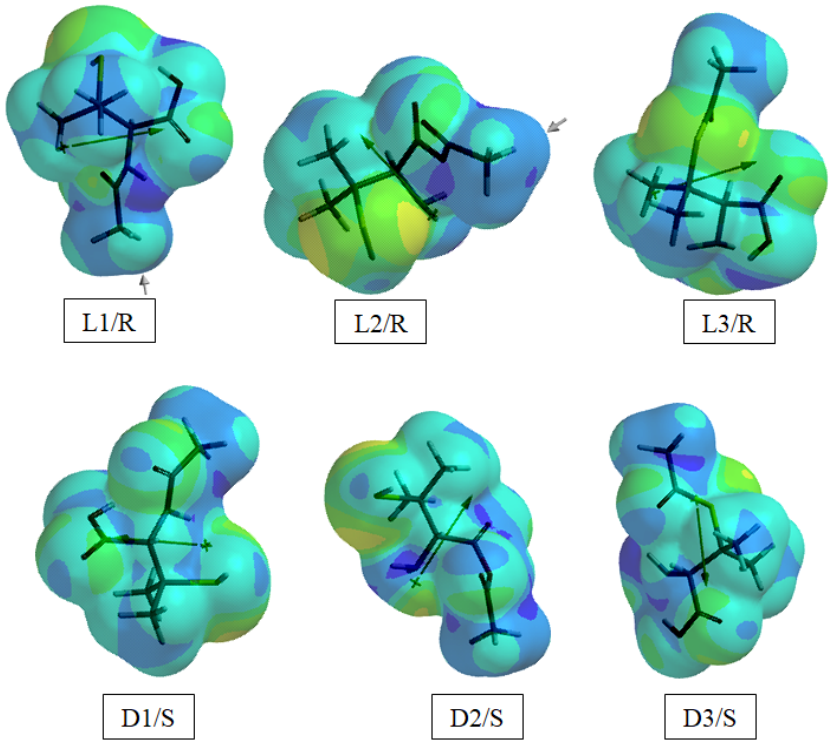

Figure 8. The local ionization potential maps of the species considered.

Figure 9 shows the LUMO maps of the isomers considered. A LUMO map displays the absolute value of the LUMO on the electron density surface. The blue color stands for the maximum value of the LUMO and the color red, the minimum value.

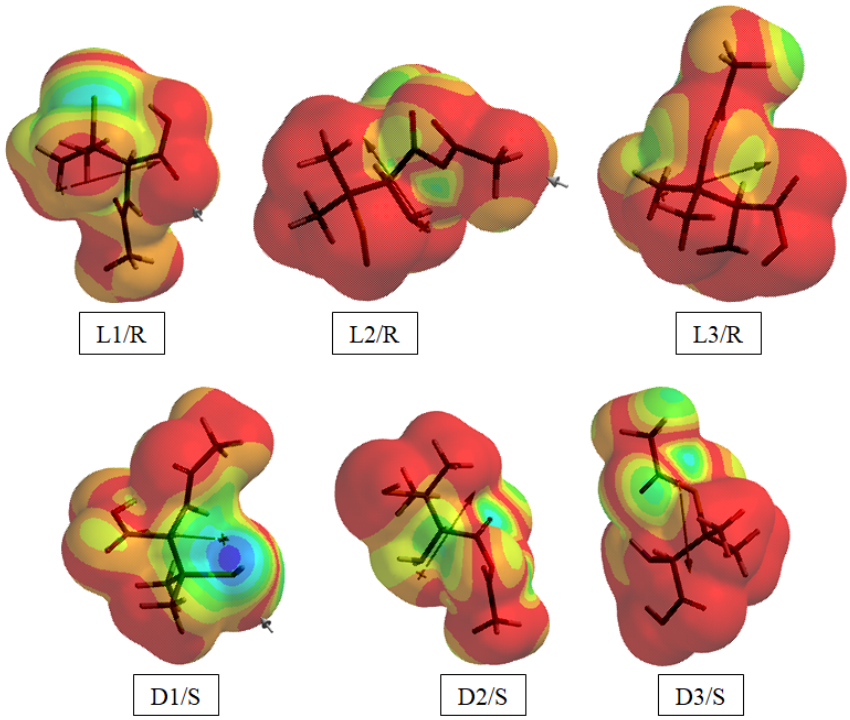

Figure 9. The LUMO maps of the species considered.

Table 6 includes the HOMO, LUMO energies and interfrontier molecular orbital energy gap values, Δε (Δε = ε_{LUMO}-ε_{HOMO}) of the structures considered. The algebraic orders of the HOMO and LUMO energies are L1/R< D1/S< D3/S< L3/R< D2/S< L2/R and D2/S< D3/S< L2/R< L3/R< D1/S< L1/R, respectively. As an outline, acetyl group lowers the HOMO energy of the molecule depending on where it is attached, namely in the order of N>S>O (irrespectful of the configuration). It reflects the order of electron withdrawing power of the acetyl group in lowering the HOMO energy level. Whereas the LUMO energies are affected as O>S having the same configuration. As for the molecular orbital energy gap values, Δε, the order is L1/R> D1/S> L3/R> D3/S> D2/S> L2/R. Energy lowering effect of any substituent is intricate function of π- and σ-electronic factors. Since in each case the acetyl group linked to a heteroatom, then π-interaction/conjugation between atoms of linkage is affected also by the sizes (size match or mismatch) of the adjacent atomic orbitals [25].

Table 6. The HOMO and LUMO energies and Δε values of the species considered.

Structure/ configuration	Acetyl linkage	HOMO	LUMO	Δε
L1/R	N-	-716.78	-76.73	640.05
L2/R	O-	-651.86	-128.45	523.41
L3/R	S-	-675.26	-93.36	581.90
D1/S	N-	-709.96	-91.14	618.82
D2/S	O-	-670.24	-140.14	530.10
D3/S	S-	-703.86	-129.40	574.46

Energies in kJ/mol.

Figure 10 is some of the molecular orbital energy levels of structures L1/R-L3/R. The overall effect of the electron attracting and donating character of the substituents shuffle the molecular orbital energy levels.

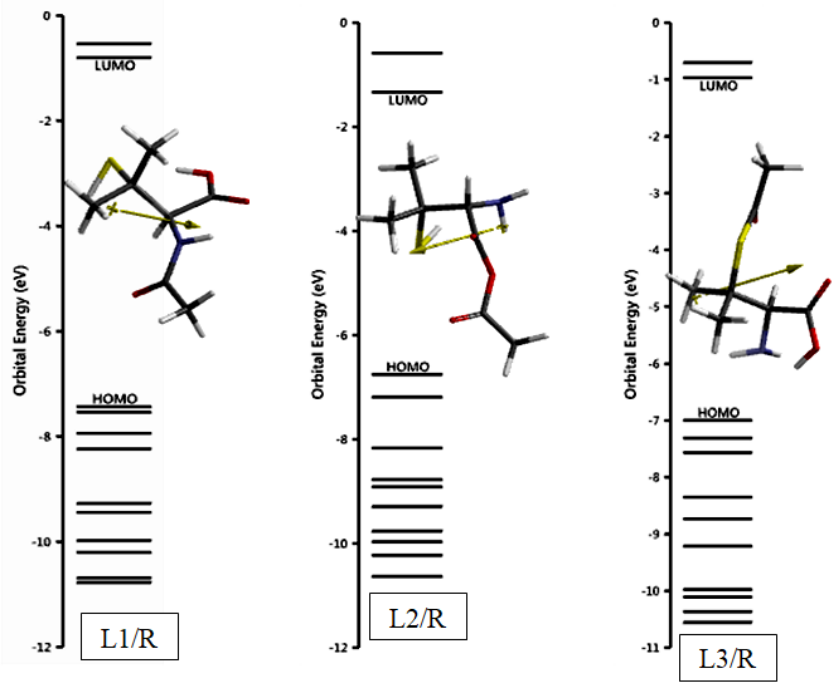

Figure 10. Some of the molecular orbital energy levels of structures L1/R-L3/R.

As seen in Figure 10, in the acetyl case, the HOMO and NEXTHOMO as well as the LUMO and NEXTLUMO energy levels are closely spaced compared to the others,

Figure 11 shows some of the molecular orbital energy levels of structures D1/S-D3/S. In the figure, the large energy spacing between the LUMO and NEXTLUMO levels in the case of O-acetyl and S-acetyl cases (the configurations are the same) is noticeable.

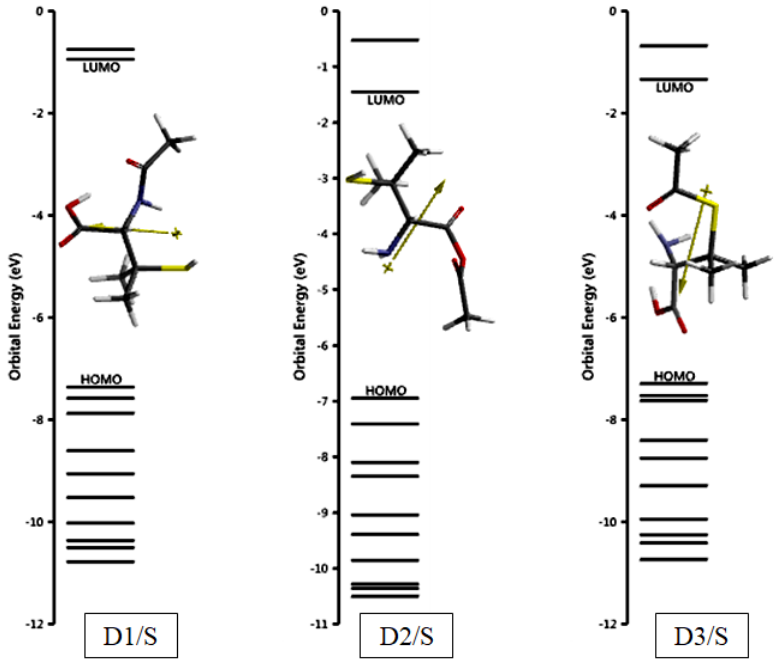

Figure 11. Some of the molecular orbital energy levels of structures D1/S-D3/S.

Figure 12 displays the calculated UV-VIS spectra (time dependent DFT, TDDFT) of the species of present interest. All the species have the spectra in the UV region below 400 nm. Structures L2/R and D2/S show a weak shoulder. Since the structures do not have a long range of π-conjugation, their spectrums are confined to UV-region only. On the other hand, the calculated intensities of the peaks are related to magnitudes of the transition moments between the orbitals involved which vary from structure to structure [26-28].

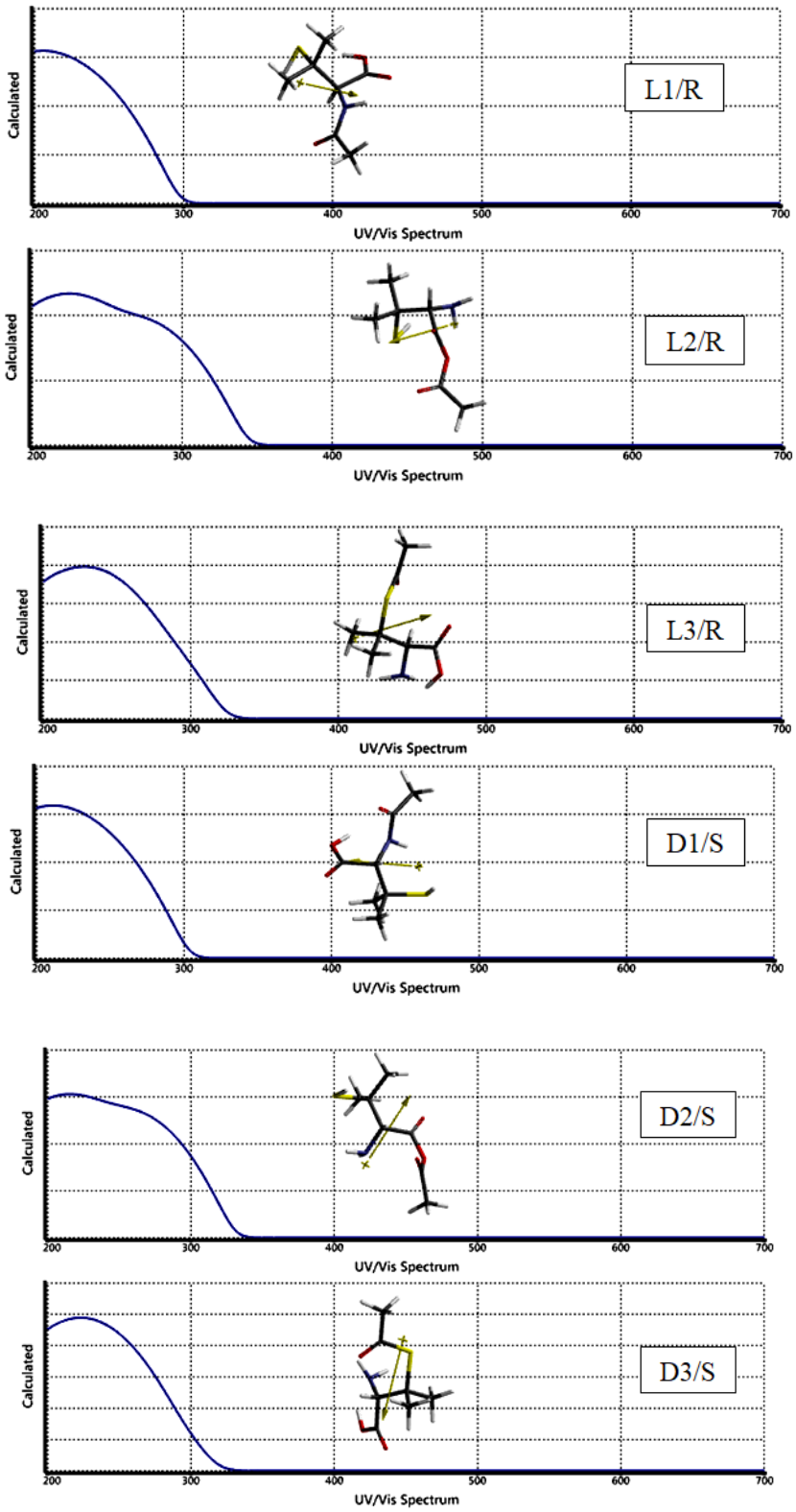

Figure 12. Calculated UV-VIS spectra of the species of present interest.

4. Conclusion

The present DFT study, within the restrictions of the density functional theory, at the level of B3LYP/6-311++G(d,p) indicates that in vacuum and aqueous conditions the dantrolene isomers have exothermic heat of formation values and favorable Gibbs free energy of formation values. All the systems considered are electronically stable.

The perturbations caused by variation of the linkage position of the acetyl moiety, thus accompanied configurational and topological changes affect many quantum chemical properties of the systems, especially the molecular orbital energy levels. However their influence on the calculated UV-VIS spectra is not drastic at all.

The present study, at the molecular level should be accompanied by some clinical investigations in order to harvest some medicinal benefits.

References

[1] Aaseth, J. (1976). Mobilization of methyl mercury in vivo and in vitro using N-acetyl-DL-penicillamine and other complexing agents. *Acta Pharmacologica et Toxicologica, 39*(3), 289–301. https://doi.org/10.1111/j.1600-0773.1976.tb03180.x

[2] Aaseth, J., Alexander, J., & Deverill, J. (1981). Evaluation of methyl mercury chelating agents using red blood cells and isolated hepatocytes. *Chemico-Biological Interactions, 36*(3), 287–297. https://doi.org/10.1016/0009-2797(81)90072-7

[3] Nielsen, J. B., & Andersen, O. (1991). Effect of four thiol-containing chelators on disposition of orally administered mercuric chloride. *Human & Experimental Toxicology, 10*(6), 423–430. https://doi.org/10.1177/096032719101000610

[4] Ogura, T., DeGeorge, G., Tatemichi, M., & Esumi, H. (1998). Suppression of anti-microtubule agent-induced apoptosis by nitric oxide: Possible mechanism of a new drug resistance. *Japanese Journal of Cancer Research, 89*(2), 199–205. https://doi.org/10.1111/j.1349-7006.1998.tb00549.x

[5] Takhampunya, R., Padmanabhan, R., & Ubol, S. (2006). Antiviral action of nitric oxide on dengue virus type 2 replication. *Journal of General Virology, 87*(Pt 10), 3003–3011. https://doi.org/10.1099/vir.0.81880-0

[6] Fenton, E. D. (1995). Biocoordination chemistry. Oxford Science Publications.

[7] Zhang, Y., & Hogg, N. (2005). S-nitrosothiols: Cellular formation and transport. *Free Radical Biology and Medicine, 38*(7), 831–838. https://doi.org/10.1016/j.freeradbiomed.2004.12.016

[8] Refsvik, T. (1984). N-acetylpenicillamine potentiated excretion of methyl mercury in rat bile: Influence of S-methylcysteine. *Acta Pharmacologica et Toxicologica, 55*, 121–123.

[9] Refsvik, T. (1987). Metabolization of 14C-N-acetylpenicillamine and 14C-cysteine in relation to 1-chloro-2,4-dinitrobenzene and sulphobromophthalein conjugation and biliary excretion in the rat. *Pharmacology & Toxicology, 60*(2), 125–128. https://doi.org/10.1111/j.1600-0773.1987.tb01510.x

[10] Refsvik, T. (1984). N-acetylpenicillamine potentiation of biliary excretion of methyl mercury: Influence of glutathione depletors. *Acta Pharmacologica et Toxicological, 55*(1), 58–64. https://doi.org/10.1111/j.1600-0773.1984.tb01962.x

[11] Pilkington, A. E., & Waring, R. H. (1988). The metabolism and disposition of D-penicillamine in the DA-strain rat. *European Journal of Drug Metabolism and Pharmacokinetics, 13*(2), 99–104. https://doi.org/10.1007/BF03191310

[12] Gupta, A., Sen, S. M., Kumar, A., Meena, K., Baishya, B., Mathias, A., Mishra, A. K., Rao, N. K., Singh, N., & Singh, P. (2024). Probing and gauging of D-penicillamine xenobiotics in hepatic Wilson disease patients. *Biophysical Chemistry, 313*, 107306. https://doi.org/10.1016/j.bpc.2024.107306

[13] Isamy, N., Bohle, D. S., Butt, J. A., Irvine, G. J., Jordan, P. A., & Sagan, E. (1999). Interrelationships between conformational dynamics and the redox chemistry of S-nitrosothiols. *Journal of the American Chemical Society, 121*(30), 7115–7123. https://doi.org/10.1021/ja9901314

[14] Stewart, J. J. P. (1989). Optimization of parameters for semi-empirical methods I. *Journal of Computational Chemistry, 10*, 209–220. https://doi.org/10.1002/jcc.540100208

[15] Stewart, J. J. P. (1989). Optimization of parameters for semi-empirical methods II. *Journal of Computational Chemistry, 10*, 221–264. https://doi.org/10.1002/jcc.540100209

[16] Leach, A. R. (1997). *Molecular modeling*. Longman.

[17] Kohn, W., & Sham, L. J. (1965). Self-consistent equations including exchange and correlation effects. *Physical Review, 140*, A1133–A1138. https://doi.org/10.1103/PhysRev.140.A1133

[18] Parr, R. G., & Yang, W. (1989). *Density functional theory of atoms and molecules*. Oxford University Press.

[19] Becke, A. D. (1988). Density-functional exchange-energy approximation with correct asymptotic behavior. *Physical Review A, 38*, 3098–3100. https://doi.org/10.1103/PhysRevA.38.3098

[20] Vosko, S. H., Wilk, L., & Nusair, M. (1980). Accurate spin-dependent electron liquid correlation energies for local spin density calculations: A critical analysis. *Canadian Journal of Physics, 58*, 1200–1211. https://doi.org/10.1139/p80-159

[21] Lee, C., Yang, W., & Parr, R. G. (1988). Development of the Colle-Salvetti correlation energy formula into a functional of the electron density. *Physical Review B, 37*, 785–789. https://doi.org/10.1103/PhysRevB.37.785

[22] Wavefunction Inc. (2006). SPARTAN 06.

[23] Hitchcock, S. A., & Pennington, L. D. (2006). Structure–brain exposure relationships. *Journal of Medicinal Chemistry, 49*(26), 7559–7583. https://doi.org/10.1021/jm060642i

[24] Shityakov, S., Neuhaus, W., Dandekar, T., & Förster, C. (2013). Analysing molecular polar surface descriptors to predict blood-brain barrier permeation. *International Journal of Computational Biology and Drug Design, 6*(1–2), 146–156. https://doi.org/10.1504/IJCBDD.2013.052195

[25] Fleming, I. (1976). *Frontier orbitals and organic reactions*. Wiley.

[26] Turro, N. J. (1991). *Modern molecular photochemistry*. University Science Books.

[27] Barrow, G. M. (1962). *Introduction to molecular spectroscopy*. Kogakusha.

[28] Harris, D. C., & Bertolucci, M. D. (1978). *Symmetry and spectroscopy*. Oxford University Press.